Reaction Networks

International Edition: DOI: 10.1002/anie.201806944
German Edition: DOI: 10.1002/ange.201806944

Bottom-Up Construction of an Adaptive Enzymatic Reaction Network

*Britta Helwig, Bob van Sluijs, Aleksandr A. Pogodaev, Sjoerd G. J. Postma, and Wilhelm T. S. Huck**

Abstract: *The reproduction of emergent behaviors in nature using reaction networks is an important objective in synthetic biology and systems chemistry. Herein, the first experimental realization of an enzymatic reaction network capable of an adaptive response is reported. The design is based on the dual activity of trypsin, which activates chymotrypsin while at the same time generating a fluorescent output from a fluorogenic substrate. Once activated, chymotrypsin counteracts the trypsin output by competing for the fluorogenic substrate and producing a non-fluorescent output. It is demonstrated that this network produces a transient fluorescent output under out-of-equilibrium conditions while the input signal persists. Importantly, in agreement with mathematical simulations, we show that optimization of the pulse-like response is an inherent trade-off between maximum amplitude and lowest residual fluorescence.*

Living organisms have remarkable capabilities such as self-healing, adaptation to the environment, homeostasis, and converting chemical energy into motion, growth, and division. To harness these capabilities in a synthetic framework is one of the ultimate goals in the fields of synthetic biology and systems chemistry,[1,2] in which we seek inspiration from the metabolic, signaling, and genetic networks of coupled chemical reactions ubiquitous in nature.[3] These networks are often based on well-established network motifs; recurring patterns of interconnections between network components that lead to a certain dynamic behavior.[4] In recent years, striking examples of synthetic reaction networks showing impressive temporal outputs have been reported. These include the so-called repressilator network,[5] a synthetic gene oscillator based on a dual-feedback circuit,[6] spatiotemporal programmable in vitro genetic and toehold-mediated strand displacement networks,[7–9] as well as enzyme- or small molecule-based reaction networks.[10–17]

Adaptation is a type of dynamic behavior that allows a biological system to sense a persistent change in the environment, produce a transient output, and return to (nearly) basal levels of activity.[18] Signaling pathways are often characterized by adaptive responses, which can efficiently propagate signals through a network. One of the network motifs underlying this response, consisting of only three components, is the incoherent type 1 feed-forward loop (I1-FFL, Figure 1 a).[19,20] In an I1-FFL, the output is directly positively controlled by the input. This is counteracted by an indirect negative control. The time delay between the positive and negative control enables this network motif to generate a pulse-like, adaptive output in response to a persistent input (Figure 1 b).

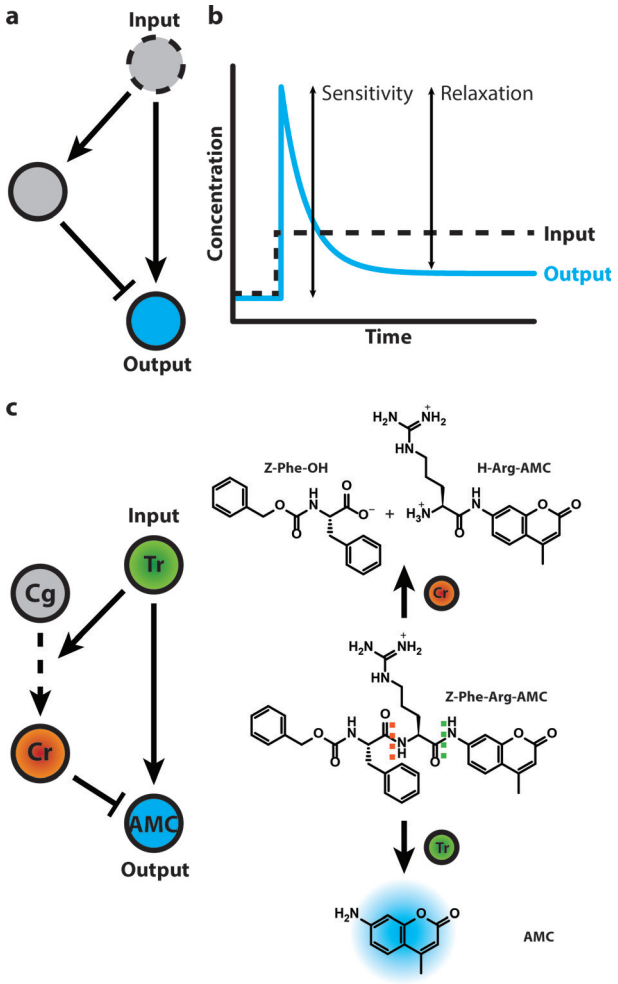

Figure 1. a) Network motif of the incoherent type 1 feed-forward loop (I1-FFL), in which the output is positively controlled in a direct manner but negatively controlled in an indirect manner. b) The typical shape of an adaptive or pulse-like response (blue line) in response to a persistent input (dashed black line). Sensitivity and relaxation are indicated by arrows. The sensitivity is a measure of the strength of the response relative to the input. Relaxation compares the steady-state response to the maximum response. c) Our adaptive enzymatic reaction network, which was inspired by the I1-FFL network motif, with trypsin (Tr) as a persistent input.

[*] B. Helwig, B. van Sluijs, A. A. Pogodaev, Dr. S. G. J. Postma, Prof. Dr. W. T. S. Huck
Radboud University, Institute for Molecules and Materials
Heyendaalseweg 135, 6525 AJ Nijmegen (The Netherlands)
E-mail: w.huck@science.ru.nl
Supporting information and the ORCID identification number(s) for the author(s) of this article can be found under: https://doi.org/10.1002/anie.201806944.

The adaptive response has been studied both in silico and experimentally. Computational studies mainly focused on the design and optimization of the adaptive response,[21–23] and demonstrated feed-forward loop-based logic gates in a systems chemistry context.[24] In addition, several experimental studies succeeded in constructing synthetic adaptive genetic networks using the I1-FFL network motif both in vivo and in vitro.[25–27] Surprisingly, as adaptation is one of the most prevalent functional modules in natural systems, the construction of adaptive enzymatic reaction networks has been lagging behind.

In contrast to genetic networks, enzymatic reaction networks encompass a wide variety of species with different activities, shapes, and sizes. Additionally, they can be applied to create functional molecular systems such as autonomously moving nanoparticles,[28] transiently self-assembling molecules that result in polymer growth and changes in supramolecular chirality,[29] responsive gels,[30–32] and reversibly forming coacervate droplets.[33] Herein, we present the first adaptive enzymatic reaction network inspired by the I1-FFL network motif (Figure 1c). In contrast to previous work in which both the input and response are transient,[14,15,17,29,32,33] our enzymatic network transiently responds to a persistent input signal that is not consumed or converted during the response. Therefore, our network is adaptive rather than only generating a pulse-like response, and its realization significantly expands the functional dynamic behaviors that can be achieved using enzymatic reaction networks.

The network is based on the endopeptidase trypsin (Tr), which acts as an input, the proenzyme chymotrypsinogen (Cg), and a fluorogenic substrate (Z-Phe-Arg-AMC). Trypsin cleaves the fluorogenic substrate, producing a short peptide fragment and the fluorescent product 7-amino-4-methylcoumarin (AMC). On a comparable timescale, Tr activates Cg, producing the active enzyme chymotrypsin (Cr). Activated Cr competes with Tr for cleavage of the fluorogenic substrate. Since Tr and Cr have different cleavage sites, the products of the cleavage by Cr are non-fluorescent, and AMC cannot be produced as a result of any further cleavage by Tr (as Tr is an endopeptidase). Importantly, to obtain the desired adaptive response, the network needs to be assembled under out-of-equilibrium conditions in a continuously stirred-tank reactor (CSTR). In a CSTR, the inflow of fresh reagents (Tr, Cg, and Z-Phe-Arg-AMC) is counterbalanced by the outflow of reagents and reaction products. Flow is herein described as k_{flow} (the ratio of the flowrate to the reactor volume) in units of h^{-1}. If the reaction rates of all the individual reactions within the network are sufficiently balanced, AMC is directly produced in response to a constant input of Tr. After some time, a sufficient amount of Cr is produced, that competes with Tr for the fluorogenic substrate, causing the concentration of AMC to decrease as all components in the CSTR are continuously refreshed. To obtain perfect adaptation, the concentration of AMC in the steady state has to be equal or close to its pre-input concentration.

To find the experimental conditions needed to obtain such a response, we determined the rates of all the known individual reactions within the network and constructed a computational model. This model, which also takes into account the flow of reactants in and out of the reactor, uses a set of ordinary differential equations (ODEs) given by the rate equations for each reaction. We subsequently searched the control parameter space (k_{flow}, [Cg], and [Tr]) in silico to determine the effect of these different parameters on the response, which was then experimentally verified. The reaction rates were optimized in silico using experimental data, and these optimized rates were used to find and test a series of optimal adaptive responses in experiments.

Figure 1c shows the enzymatic I1-FFL, using commercially available Z-Phe-Arg-AMC as a fluorogenic substrate. Trypsin, the input, cleaves amide bonds at the C-terminal end of positively charged amino acids (in this study, arginine) producing the dipeptide Z-Phe-Arg-OH and the fluorescent product AMC. Trypsin also activates Cg, thereby producing Cr. Chymotrypsin preferably cleaves amide bonds after hydrophobic, aromatic amino acids (in this study, phenylalanine), producing two fragments, Z-Phe-OH and H-Arg-AMC. We determined the catalytic efficiencies (k_{cat}/K_M) of enzymatic cleavage reactions by Tr and Cr to be 842 $\mu M^{-1} h^{-1}$

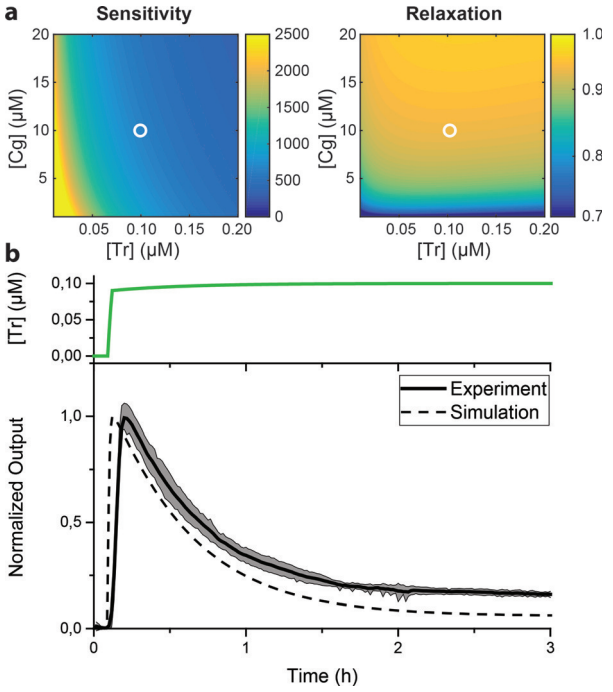

Figure 2. In silico approximated phase diagrams and the result of the corresponding experiment. a) Phase diagrams of the sensitivity and relaxation as a function [Tr] and $[Cg]_0$; $[Z\text{-Phe-Arg-AMC}]_0 = 100\ \mu M$ and $k_{flow} = 2\ h^{-1}$. Whereas the score for sensitivity increases with decreasing [Tr] and $[Cg]_0$, the score for relaxation increases with increasing [Tr] and $[Cg]_0$. Experimental conditions that would favor both were chosen (indicated by the white circle). b) Experimental results corresponding to the conditions indicated by the white circles in the phase diagrams ($[Tr] = 0.1\ \mu M$, $[Cg]_0 = 10\ \mu M$, $[Z\text{-Phe-Arg-AMC}]_0 = 100\ \mu M$, and $k_{flow} = 2\ h^{-1}$). The experiments were performed at 30 °C in buffer at pH 7.7, containing 100 mM Tris-HCl and 20 mM $CaCl_2$. The top graph shows the stepwise increase in [Tr]. The solid black line in the bottom graph is the average response of six experiments; the shaded area indicates the standard deviation of the response. Simulations of the response using the same initial conditions are given by the dashed black line.

and 720 $\mu M^{-1} h^{-1}$, respectively, indicating that Tr and Cr cleave Z-Phe-Arg-AMC at comparable rates. We measured a value for k_{cat}/K_M of 8 $\mu M^{-1} h^{-1}$ for the activation of Cg by Tr, creating a somewhat delayed indirect negatively controlled node in our network (Section S2 of the Supporting Information).

With these rates we could approximate the phase diagrams of this network in silico (Figure 2a). These diagrams depict the sensitivity and relaxation (Figure 1b), which are the two characteristics that we used to quantify the response of our network, as a function of [Tr] and $[Cg]_0$. For practical reasons, we fixed the $[Z\text{-Phe-Arg-AMC}]_0$ at 100 μM and set k_{flow} at 2 h^{-1}. The corresponding scoring functions for sensitivity and relaxation related to the response of the network as depicted in Figure 1b are defined, respectively, in Equations (1) and (2):

$$\text{Sensitivity} = \frac{\text{Output}(t = \text{maximum response})}{\Delta\text{Input}} \quad (1)$$

$$\text{Relaxation} = 1 - \frac{\text{Output}(t = \text{steady state})}{\text{Output}(t = \text{maximum response})} \quad (2)$$

A high score for sensitivity corresponds to a high initial response relative to the input, whereas a high score for relaxation indicates that the response of the network returns close to pre-input levels (Section S4.2.4 of the Supporting Information). The phase diagrams in Figure 2a show that the score for sensitivity increases with a decrease in [Tr] and $[Cg]_0$, whereas the score for relaxation increases with an increase in [Tr] and $[Cg]_0$. This demonstrates that these characteristic quantities are competing objectives.

We opted for experimental conditions that would favor both sensitivity and relaxation more or less equally. A fully transparent CSTR, which was fabricated from polydimethylsiloxane and bonded onto a glass slide, was used to carry out the experiment. The production of AMC in the CSTR was measured directly through the glass slide using fluorescence readout (Section S3 of the Supporting Information). We tested our network experimentally under flow conditions using [Tr] = 0.1 μM and $[Cg]_0$ = 10 μM, as indicated by the white circles in Figure 2a. In accordance with model simulations, a steep initial rise in fluorescence intensity, corresponding to the production of AMC, was followed by a more gradual decrease (Figure 2b). A stable steady state was reached after between 2.5 and 3 h.

Encouraged by these results, we probed the effect of different control parameters (k_{flow}, $[Cg]_0$, and [Tr]) on the sensitivity, relaxation, and shape of the peak. We observed experimentally that k_{flow} mainly has an effect on the timescale of the adaptive response, where higher values for k_{flow} result in a faster response with comparable sensitivity and relaxation (Figure 3a). Changing $[Cg]_0$ has a bigger effect on the sensitivity than on the relaxation (Figure 3b), whereas changing [Tr] has an effect on both the sensitivity and relaxation (Figure 3c). Increasing $[Cg]_0$ worsens the sensitivity, whereas the relaxation remains more or less the same. Increasing [Tr] also worsens the sensitivity of the response, as the increase in amplitude does not scale linearly with the increase in [Tr] (Section S3.4 of the Supporting Information). Again, the obtained experimental results are in good agreement with model simulations, although the relaxation deviates from what was expected based on the model. These

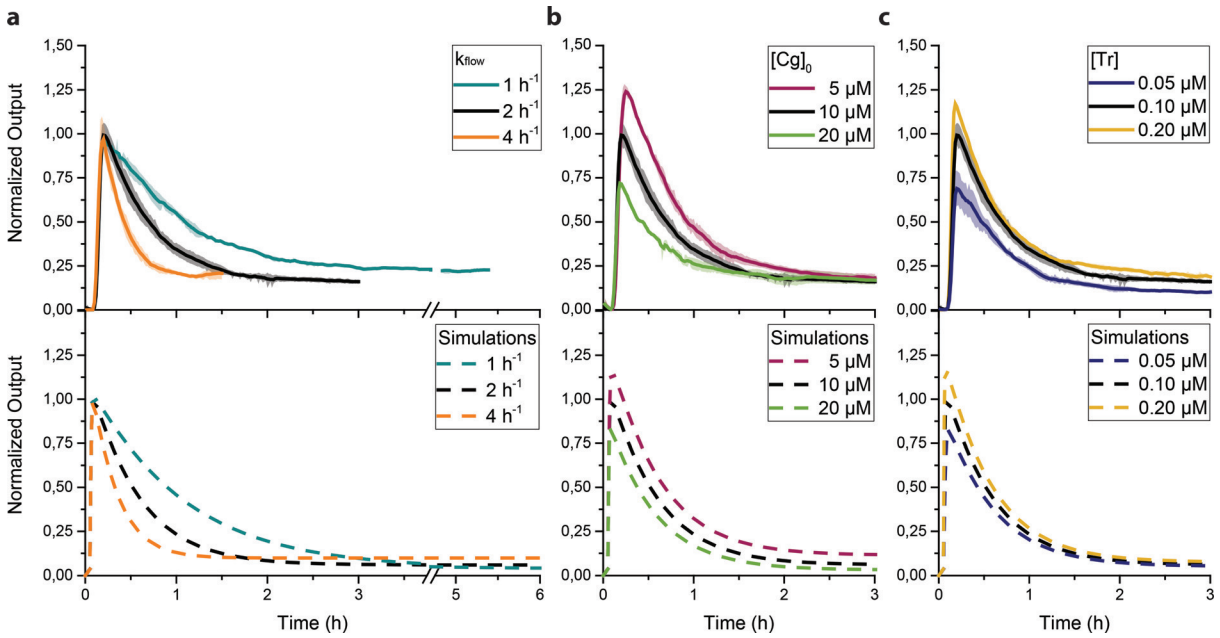

Figure 3. The effect of k_{flow}, $[Cg]_0$, and [Tr] on network response. Top figures (solid lines) show the experimental results and the bottom figures (dashed lines) show simulations. a) Effect of k_{flow} (k_{flow} = 1 h^{-1}, 2 h^{-1}, and 4 h^{-1}); [Tr] = 0.1 μM, $[Cg]_0$ = 10 μM, and $[Z\text{-Phe-Arg-AMC}]_0$ = 100 μM. b) Effect of $[Cg]_0$ ($[Cg]_0$ = 5 μM, 10 μM, and 20 μM); [Tr] = 0.1 μM, $[Z\text{-Phe-Arg-AMC}]_0$ = 100 μM, and k_{flow} = 2 h^{-1}. c) Effect of [Tr] ([Tr] = 0.05 μM, 0.10 μM, and 0.20 μM); $[Cg]_0$ = 10 μM, $[Z\text{-Phe-Arg-AMC}]_0$ = 100 μM, and k_{flow} = 2 h^{-1}. All experiments (except [Tr] = 0.1 μM, $[Cg]_0$ = 10 μM, $[Z\text{-Phe-Arg-AMC}]_0$ = 100 μM, and k_{flow} = 2 h^{-1}, which was performed six times) were performed in triplicate at 30 °C in buffer of pH 7.7 containing 100 mM Tris-HCl and 20 mM $CaCl_2$.

results demonstrate that an adaptive response is obtained within a relatively broad parameter space, which means the network is parametrically robust (Section S4.3 of the Supporting Information).[34]

Next, we re-estimated the set of reaction rates using data from the previous experiments to improve our computational model. The control parameters (parameters that can be experimentally controlled, that is, k_{flow}, [Tr], $[Cg]_0$, and [Z-Phe-Arg-AMC]$_0$) were evolved for a series of optimally sensitive and relaxed responses (using an evolutionary algorithm, Section S4.2 of the Supporting Information), taking into account experimental feasibility (e.g. solubility of Z-Phe-Arg-AMC, timescale of the reaction). The result of this optimization is a two-dimensional Pareto front (Figure 4a), in which each point represents a set of conditions for which the relaxation cannot be improved without negatively impacting the sensitivity and vice versa. Upon closer inspection, we found that the k_{flow} and [Z-Phe-Arg-AMC]$_0$ were evolved towards their lower and upper boundaries, respectively. Therefore, within these experimental constraints, sensitivity and relaxation are tuned by the ratio between [Tr] and $[Cg]_0$ (Figure 4b). Finally, we tested several points along this Pareto front experimentally (Figure 4c), demonstrating that we can optimize the response of the network precisely and tune it to suit the needs that future applications might require.

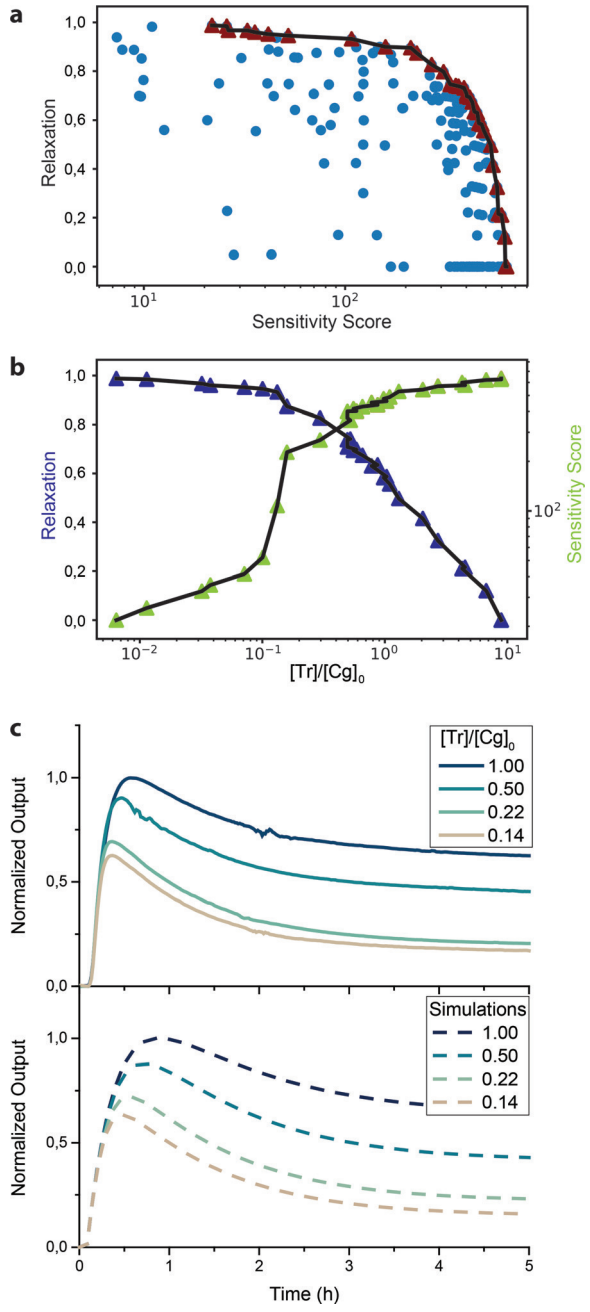

Figure 4. a) Pareto front for sensitivity and relaxation. The red triangles represent sets of optimal conditions (taking into account experimental constraints such as solubility of Z-Phe-Arg-AMC and feasible values for k_{flow}). The blue dots represent non-optimal solutions. Concentration profiles can be found in Figure S12 of the Supporting Information. b) Influence of [Tr]/$[Cg]_0$ on the sensitivity and relaxation; [Z-Phe-Arg-AMC]$_0$ = 100 μM (the upper boundary) and k_{flow} = 1 h^{-1} (the lower boundary). c) Experimental results representing points on the Pareto front, where [Tr]/$[Cg]_0$ was varied by keeping [Tr] fixed at 1 μM and varying $[Cg]_0$.

In summary, we constructed a well-characterized adaptive enzymatic reaction network based on the I1-FFL network motif. Combining kinetic studies of all individual reactions within the network with a computational approach proved successful for obtaining the desired pulse-like network response experimentally. We demonstrated that the sensitivity and relaxation of this response, which can be found within a broad parameter space, can be modified by varying different control parameters. We believe that the functionality of this network can be extended by creating molecular logic gates through changing the enzymatic recognition sites of the substrate, by replacing AMC with a functional moiety that is released in a pulse-like manner and influences the behavior of other reaction networks, or by embedding it in materials for applications such as edge-detection.[35]

Acknowledgements

This work was supported by funding from the Dutch Ministry of Education, Culture and Science (Gravity program 024.001.035).

Conflict of interest

The authors declare no conflict of interest.

Keywords: adaptation · enzymes · kinetics · out-of-equilibrium processes · reaction networks

How to cite: *Angew. Chem. Int. Ed.* **2018**, *57*, 14065–14069
Angew. Chem. **2018**, *130*, 14261–14265

[1] S. A. Benner, A. M. Sismour, *Nat. Rev. Genet.* **2005**, *6*, 533.
[2] G. Ashkenasy, T. M. Hermans, S. Otto, A. F. Taylor, *Chem. Soc. Rev.* **2017**, *46*, 2543–2554.
[3] B. A. Grzybowski, W. T. S. Huck, *Nat. Nanotechnol.* **2016**, *11*, 585–592.

[4] R. Milo, S. Shen-Orr, S. Itzkovitz, N. Kashtan, D. Chklovskii, U. Alon, *Science* **2002**, *298*, 824 – 827.
[5] M. B. Elowitz, S. Leibler, *Nature* **2000**, *403*, 335 – 338.
[6] J. Stricker, S. Cookson, M. R. Bennett, W. H. Mather, L. S. Tsimring, J. Hasty, *Nature* **2008**, *456*, 516 – 519.
[7] A. J. Genot, A. Baccouche, R. Sieskind, N. Aubert-Kato, N. Bredeche, J. F. Bartolo, V. Taly, T. Fujii, Y. Rondelez, *Nat. Chem.* **2016**, *8*, 760.
[8] N. Srinivas, J. Parkin, G. Seelig, E. Winfree, D. Soloveichik, *Science* **2017**, *358*, eaal2052.
[9] E. Karzbrun, A. M. Tayar, V. Noireaux, R. H. Bar-Ziv, *Science* **2014**, *345*, 829 – 832.
[10] S. N. Semenov, A. S. Y. Wong, R. M. van der Made, S. G. J. Postma, J. Groen, H. W. H. van Roekel, T. F. A. de Greef, W. T. S. Huck, *Nat. Chem.* **2015**, *7*, 160 – 165.
[11] S. G. J. Postma, D. te Brinke, I. N. Vialshin, A. S. Y. Wong, W. T. S. Huck, *Tetrahedron* **2017**, *73*, 4896 – 4900.
[12] S. N. Semenov, L. J. Kraft, A. Ainla, M. Zhao, M. Baghbanzadeh, V. E. Campbell, K. Kang, J. M. Fox, G. M. Whitesides, *Nature* **2016**, *537*, 656 – 660.
[13] T.-R. Chen, C.-F. Hsu, C.-L. Chen, H. A. Witek, P. L. Urban, *ACS Synth. Biol.* **2016**, *5*, 962 – 968.
[14] C. Pezzato, L. J. Prins, *Nat. Commun.* **2015**, *6*, 7790.
[15] Y. Zhang, S. Tsitkov, H. Hess, *Nat. Catal.* **2018**, *1*, 276 – 281.
[16] J. W. Sadownik, T. Kosikova, D. Philp, *J. Am. Chem. Soc.* **2017**, *139*, 17565 – 17573.
[17] J. P. Wojciechowski, A. D. Martin, P. Thordarson, *J. Am. Chem. Soc.* **2018**, *140*, 2869 – 2874.
[18] J. E. Ferrell, *Cell Syst.* **2016**, *2*, 62 – 67.
[19] U. Alon, *Nat. Rev. Genet.* **2007**, *8*, 450.
[20] W. Ma, A. Trusina, H. El-Samad, W. A. Lim, C. Tang, *Cell* **2009**, *138*, 760 – 773.
[21] H. W. H. van Roekel, L. H. H. Meijer, S. Masroor, Z. C. Félix Garza, A. Estévez-Torres, Y. Rondelez, A. Zagaris, M. A. Peletier, P. A. J. Hilbers, T. F. A. de Greef, *ACS Synth. Biol.* **2015**, *4*, 735 – 745.
[22] Y. Boada, G. Reynoso-Meza, J. Picó, A. Vignoni, *BMC Syst. Biol.* **2016**, *10*, 27.
[23] R. W. Smith, B. van Sluijs, C. Fleck, *BMC Syst. Biol.* **2017**, *11*, 118.
[24] N. Wagner, G. Ashkenasy, *Chem. Eur. J.* **2009**, *15*, 1765 – 1775.
[25] S. Basu, R. Mehreja, S. Thiberge, M.-T. Chen, R. Weiss, *Proc. Natl. Acad. Sci. USA* **2004**, *101*, 6355 – 6360.
[26] T. J. Strovas, A. B. Rosenberg, B. E. Kuypers, R. A. Muscat, G. Seelig, *ACS Synth. Biol.* **2014**, *3*, 324 – 331.
[27] J. Kim, I. Khetarpal, S. Sen, R. M. Murray, *Nucleic Acids Res.* **2014**, *42*, 6078 – 6089.
[28] M. Nijemeisland, L. K. E. A. Abdelmohsen, W. T. S. Huck, D. A. Wilson, J. C. M. van Hest, *ACS Cent. Sci.* **2016**, *2*, 843 – 849.
[29] A. Sorrenti, J. Leira-Iglesias, A. Sato, T. M. Hermans, *Nat. Commun.* **2017**, *8*, 15899.
[30] E. Jee, T. Bánsági, A. F. Taylor, J. A. Pojman, *Angew. Chem. Int. Ed.* **2016**, *55*, 2127 – 2131; *Angew. Chem.* **2016**, *128*, 2167 – 2171.
[31] S. G. J. Postma, I. N. Vialshin, C. Y. Gerritsen, M. Bao, W. T. S. Huck, *Angew. Chem. Int. Ed.* **2017**, *56*, 1794 – 1798; *Angew. Chem.* **2017**, *129*, 1820 – 1824.
[32] L. Heinen, T. Heuser, A. Steinschulte, A. Walther, *Nano Lett.* **2017**, *17*, 4989 – 4995.
[33] K. K. Nakashima, J. F. Baaij, E. Spruijt, *Soft Matter* **2018**, *14*, 361 – 367.
[34] A. S. Y. Wong, A. A. Pogodaev, I. N. Vialshin, B. Helwig, W. T. S. Huck, *J. Am. Chem. Soc.* **2017**, *139*, 8146 – 8151.
[35] S. M. Chirieleison, P. B. Allen, Z. B. Simpson, A. D. Ellington, X. Chen, *Nat. Chem.* **2013**, *5*, 1000.

Manuscript received: June 15, 2018
Revised manuscript received: August 13, 2018
Accepted manuscript online: September 5, 2018
Version of record online: October 1, 2018

